

Evaluation of the Wear-Corrosion Process in Beta-Tricalcium (β -TCP) Films Obtained by Physical Vapor Deposition (PVD)

J. Bautista-Ruiz^a, J.C. Caicedo^b, W. Aperador^c

^a Department of Electromechanical Engineering, Universidad Francisco de Paula Santander, San José de Cúcuta, Colombia,

^b Tribology, Polymers, Powder Metallurgy and Processing of Solid Recycled Research Group, Universidad del Valle, Cali, Colombia,

^c School of Engineering, Universidad Militar Nueva Granada, Bogotá, Colombia.

Keywords:

Synergy
Tricalcium phosphate
Corrosion
Coefficient of friction
PVD

ABSTRACT

A simultaneous evaluation was done of the wear-corrosion of the coatings of beta-tricalcium phosphate on titanium (Ti) substrate deposits obtained by the magnetron sputtering technique. The characterization was developed by a tribometer system coupled to an electrochemical cell. This system allows the combination of corrosion and friction tests between the surface of the coating and the spherical bone pin. The synergy of the two wear phenomena was characterized, which were monitored by means of the electrochemical response as a function of the value of the friction coefficient. It was determined that the system generates a gradual film accumulation process, followed by an instantaneous loss after a critical period. Additionally, it is concluded that the increase in the coefficient of friction is not immediately followed by the increase in wear rate.

Corresponding author:

Jorge Bautista-Ruiz
Department of Electromechanical Engineering, Universidad Francisco de Paula Santander, Avenida Gran Colombia No. 12E-96, San José de Cúcuta, Colombia.
E-mail: g.ing.materiales@gmail.com

© 2019 Published by Faculty of Engineering

1. INTRODUCTION

The inorganic portion of the bone is primarily composed of calcium and phosphate characterized as hydroxyapatite (HA) crystal with small amounts of fluorides that foster crystallization and hardening of the bones [1-3].

The last decade has seen the development of new types of materials referred to as biomaterials [4-5]. Broadly speaking, biomaterials are designed to interact with biological systems for the purpose of

treating, augmenting or replacing some tissue, organ or body function [6]. The main applications of these materials include the replacement and repair of bones, external joints, dental implants, screws and hooks to components of artificial hearts [7]. Biomaterials are biodegradable, have adequate mechanical strength, good resistance to fatigue, adequate density and weight, resistance to high impact efforts, among other characteristics [8].

Most ceramic materials are biocompatible. These materials are classified into 3 types: bio-energies,

bioactive and bioresorbable [9]. Examples of ceramic bio-energies include alumina, zirconia and carbonaceous materials [10-11]. Bioactive ceramics include hydroxyapatite, bio-glass and some vitro-ceramics [12]. Tricalcium phosphate and calcium sulfates are examples of bioresorbable ceramics [13].

Beta-tricalcium phosphate (β -TCP) is a high temperature phase. It is obtained at temperatures above 800 °C by thermal decomposition of calcium-deficient hydroxyapatite or by interaction in the solid state of acidified calcium orthophosphate [14]. β -TCP cannot be precipitated from aqueous solutions. In addition to the chemical preparation routes, β -TCP with substituted ions can be prepared through the calcination of bones. At temperatures above 1125 °C, β -TCP reaches a stable phase - α -TCP [15]. However, the ideal structures of β -TCP have gaps of calcium ions, which can be occupied with magnesium ions stabilizing the structure. Pure β -TCP never occurs in biological calcifications. Only the ceramics substituted by Mg form the so-called (β -tricalcium-magnesium phosphate), β - (Ca, Mg)₃(PO₄)₂, found in dental calculus and urinary stones, cartilage with arthritis, etc. This crystal, however, is not found in enamel, dentin, or bones. In biomaterials, β -TCP is used in calcium phosphate cements [16].

Combined with HA, β -TCP forms a biphasic calcium phosphate (BCP). Both β -TCP and BCP are classified as bio-ceramic, widely used as bone tissue replacements [17]. Other uses of β -TCP include tooth polishing pastes and polyvitamin complexes [18].

The potential for the technological application of beta-tricalcium phosphate is not limited to biotechnology and medicine [19]. In the area of environmental control, the material is proposed as an absorber of heavy metals in industrial waste and contaminated water, and as a catalyst in the decomposition of organochlorine compounds pollutants from the metallurgical industry and the incineration of industrial waste [20]. On the other hand, inert ceramics have durability, stability and little or no reactivity with the tissues where they are implanted. There is minimal negative physiological response of the organism to the presence of this material [21].

Bio-ceramics with an active surface have a stable chemical bond with the host [22]. They are recommended in places where there is a need to stimulate bone growth or other tissues and, as a filler in the form of powder [23]. A classic example of an absorbable bio-ceramic is tricalcium phosphate which is usually biocompatible and easily absorbed by natural metabolism. Initially, it has low porosity, but this gradually increases allowing the tissue to grow inside the pores [24].

In surgical implants, corrosion can be a critical phenomenon, affecting both the biocompatibility of the implant and the structural integrity of the prosthesis. Corrosion and dissolution of the surface layers of the material are two mechanisms that can lead to the introduction of metal ions into the human body, causing adverse effects due to their biological reaction [25-26].

Therefore, it is proposed with this investigation to study the performance of the coatings of beta-tricalcium phosphate on Ti Substrate when subjected to both wear and corrosion, and to evaluate the biocompatibility behaviour.

2. METHODS AND MATERIALS

Thin beta-tricalcium phosphate films were deposited on Ti Substrate for the purpose of improving the mechanical and tribological properties of the substrate. The thin films were deposited by Radio Frequency (RF) magnetron-sputtering method by 5 hours. These coatings were obtained using tricalcium white phosphate with a diameter of 10 cm. The plasma conditions were: pressure of 5.21×10^{-3} mbar, current and discharge power of 250 mA and 400 W, respectively. An argon flux of 9 sccm was used. All coatings were deposited at a distance of 4 cm, substrate-target. In addition, a 100 nm thick titanium film was deposited between the substrate and the coating to improve adhesion.

The surface characterization of the coating was performed by FEI Tecani F20 electronic microscope FEG-TEM operating at 5 kV. Structural characterization was analysed by X-Ray diffraction (XRD) with a Philips X-ray diffractometer, with Bragg-Brentano configuration ($\theta / 2\theta$) in the ground beam mode, Cu K α radiation ($\lambda = 1.5405 \text{ \AA}$). Information

about crystallinity and changes in crystal lattice arrangements were obtained from diffraction patterns as a function of the increase in Chitosan concentration from β -TCP coatings.

In the evaluation of corrosion resistance under tribocorrosion conditions, a potentiostat / galvanostat was used together with an impedance analyzer suitable for a nanovea MT60 tribometer with a sliding pattern of bone, with a diameter of 6 mm and normal load of 5 N, velocity of 5 m/s and total sliding length of 80 m. An evaluation of deterioration was obtained by measuring polarization curves and corrosion resistance. As a working electrolyte, a solution composed of water, dissolved oxygen, proteins and chloride ions was used in the quantities recorded in Table 1. This solution is similar to human body fluids in order to simulate an adverse working environment for the system.

Table 1. Chemical composition of the electrolyte.

Component of solution	NaCl	KCl	CaCl ₂ ·2H ₂ O	Sodium lactate
Concentration (g/l)	6	0.30	0.22	3.10

An electrolytic solution at 37 °C was used for the electrochemical impedance spectroscopy tests (EIS). The samples remained immersed for 3 months and were evaluated at times of 0, 720, 1440 and 2160 hours, respectively. The EIS technique is not destructive and allows for the estimation of the polarization resistance value correlating it with the degree of deterioration of the sample as a function of time and change in the roughness generated by wear when using the tribometer. The EIS data were obtained in the potential open circuit configuration (OCP) stabilizing the corrosion potential. We used an electrochemical cell formed by three electrodes, a platinum counter electrode (CE), as a reference electrode silver / silver chloride (WE) and as a working electrode the coated substrates. The work area was 1.19 cm². The Nyquist graphs were obtained in frequency ranges from 0.001 Hz to 100 kHz and 15 mV amplitude of the sinusoidal signal. In order to determine the corrosion measurement, the polarization measurements were made after 2160 hours. The test time of the samples was 120 minutes immersed in balanced salt solution and scanning speed of 1mV/s. The materials were anodic polarized at - 0.25 V Ag/AgCl.

3. RESULTS

In Fig. 1, the diffractograms with the preferential orientations that correspond to the ceramic phase of the β -TCP coating are observed. These orientations present a rhombohedral system. The figure shows the orientations of the crystallographic planes identified by the Miller indices: (300), (128), (1211) (1321), (502), (2020), (508), (514) and (600) for 2 θ between 0° and 80°. The results of the XRD show greater intensity of the peaks at angles of 2 θ = 31.86°, 39.01° and 59.81° in relation to the higher concentrations of chitosan that make up the coatings. In addition, Fig. 1 shows a relationship between the percentage of chitosan, generated in the film forming process, and the intensity of the peaks. The diffraction pattern suggests an inverse proportionality relationship between the percentage of polysaccharides and the peak intensity, due to the inclusion of chitosan in the structure of β -TCP [27]. This shows that the variation in shape and size of the characteristic peaks, and the decrease in peak area and height, is a function of the percentage of the cross-linking reaction of the polysaccharides.

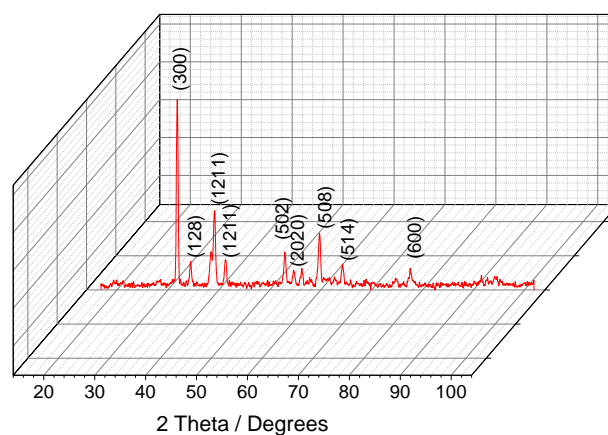


Fig. 1. X-ray diffractogram corresponding to solid sample obtained by magnetron-sputtering and peaks corresponding to the planes of the ceramic phase of the β -TCP coating.

The Figure 2 shows the cross-sectional micrographs of the Beta phosphate coating deposited on silicon substrates (100) to verify structural growth. The morphology of the coating and the quality of the adhesion at the substrate-coating interface can be observed. The micrograph makes it possible to distinguish the laminar growth of the film due to the compounds of the material that make it up [28]. In all the coatings, a first layer of Titanium was

deposited to reduce residual stress the tensions generated by the structural difference between the substrate and the ceramic layer.

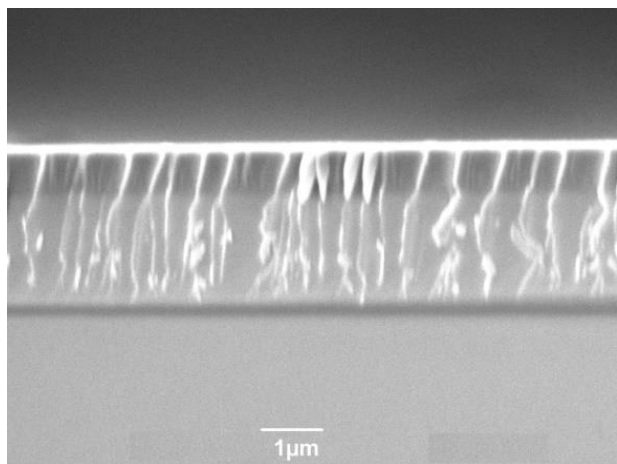


Fig. 2. Micrograph of scanning electron microscopy of the cross section of β -TCP coating deposited on silicon substrate.

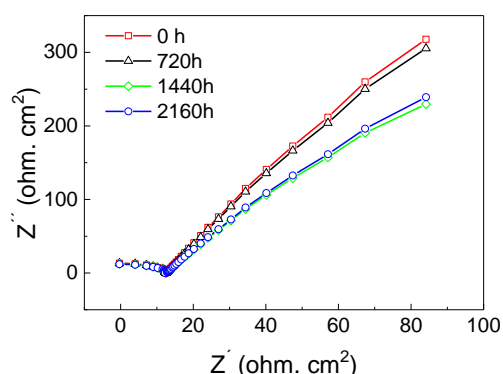


Fig. 3. Impedance graph of the β -TCP coating.

The Figure 3 shows the Nyquist diagrams as a function of time, the results allow for the analysis of the coating wear-corrosion process [29]. The impedance values were taken after stabilizing the corrosion potential (E_{corr}) for 24 hours. Measurements were made at 0, 720, 1440 and 2160 hours, respectively. The temperature was kept constant at 37 °C, to simulate the conditions of the human body, by immersing the electrochemical cell in a thermostated bath circulator [30].

The results (Fig. 3) allow establishing in the X axis the first inflection corresponding to the resistance of the electrolyte; all the studied systems overlapped indicating identical value as a function of the evaluation times. The first resistance of the system indicated an opposition to the mobility of the ions of the solution through the coating the value of which is

independent of the evaluation time. The impedance generated by the beta tricalcium phosphate coating causes two types of electrical phenomena: one represented in the two inflections at 12 ohm cm^2 and the other related to the response of the substrate-coating system where the values vary according to the evaluation time [31].

The Figure 4 shows the equivalent circuit representing the electrical characteristics of the systems evaluated by the wear-corrosion mechanism. These electrical elements permitted the simulation of the results obtained at different times of evaluation of the coatings. R_{soln} corresponds to the resistance of the solution with a value around 12 ohm cm^2 , in the four evaluation times. R_{po} is the resistance to polarization, C_c and C_{cor} are elements of constant phase, and R_{cor} is the resistance to corrosion. The set of devices contributes to a sum of impedances generating different values for each of the evaluated times. This diversity of values is associated with the reactions generated on the surface of the coating and increases its value when developing the dual test with the tribometer and the electrolyte [32]. A similar behaviour is observed between 0 and 720 hours with a total impedance value of 320 ohm cm^2 . After 1440 hours the impedance value decreases to 290 ohm cm^2 , due to the loss of the protective layer and the absorption of some component species of the electrolyte. At 2160 hours the dual corrosion-wear test system was stabilized and remained constant [33].

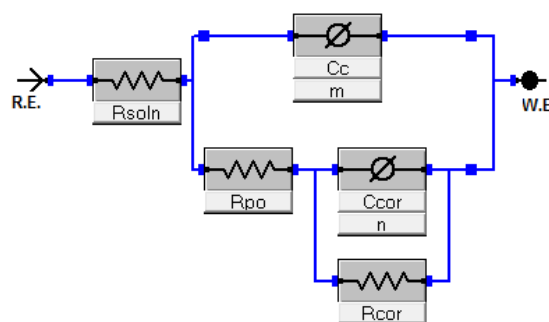


Fig. 4. Equivalent electrical circuit for electrochemical impedance spectroscopy analysis.

The potentiodynamic polarization curves observed in Fig. 5 allow for the calculation of the change generated in the coating surface caused by the wear-corrosive phenomenon. The dissolution of β -tricalcium phosphate is determined, similar to the results obtained in

the total impedance evaluation. This behaviour may indicate that the coating confers an excellent corrosion resistance when in contact with the electrolytic solution. However, when evaluating the coating system as a function of time, acceleration 5 times greater than the corrosion rate is evident for a period of 2160 hours (Table 2). This behaviour is explained by the load and accelerated dissolution conditions that result in increased velocities as a function of the evaluation time [34]. Additionally, due to the columnar structure present in the films, wear in this type of materials is compromised. The shape of the cathodic polarization curves is such that the spontaneous formation of a thin layer of oxide on the surface of the coatings can be deduced. At a time of evaluation of 2160 hours the film alters its topography by dissolution phenomena. However, this dissolution is minimal and is related to the values in the corrosion rate. The removal of the oxide layer is due to the cyclic load during the test. The amount of ions released depends on mechanical wear for which reason the material is dissolved 5 times more up until 2160 hours of study.

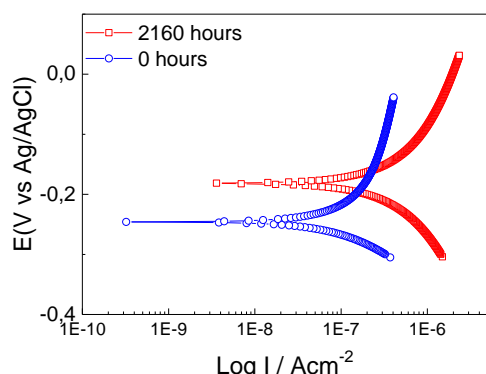


Fig. 5. Polarization curves for the coating of β -tricalcium phosphate.

Table 2. Values of corrosion current, corrosion potential and corrosion rate for β -TCP coatings evaluated at 0 hours and 2160 hours.

Parameter	2160 Hours	0 Hours
I_{corr} (μA)	100	021
E_{corr} (mV)	-182	-246
Corrosion Rate (mpy)	315	632

The Figure 6 represents the estimation of the wear rate in stable and dynamic state of the β -tricalcium phosphate films at times of 0, 720, 1440 and 2160 immersion hours. When comparing with the results of EIS, it is possible to infer that the samples evaluated at 720 hours are more resistant to wear than the samples

analysed at 1440 hours. The influence of the immersion period on the structural characteristics of the coating is then observed. This is due to the hardness of the β -TCP film and its crystalline structure [35].

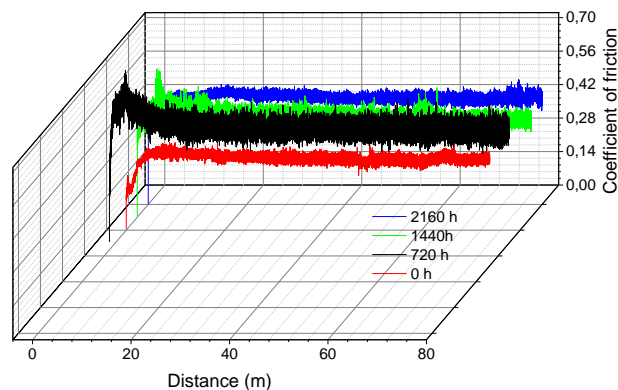


Fig. 6. Response of the average coefficient of friction as a function of the normal load, the sliding speed and the sliding distance.

As for the test to determine the coefficients of friction, the coating begins with a value of $\mu = 0.12$, contrasting this value with that obtained at 0 hours. This is explained by the low roughness of the films when produced by the magnetron sputtering technique generating homogeneous surfaces in the coating. For the other coatings evaluated, results of 0.19, 0.28 and 0.38 are obtained. This is due to the surface sprays. According to the results obtained, there is a proportional relationship between the time of immersion of the coatings and their value of the coefficient of friction. This is explained by the increase in surface roughness in the films due to the attack of the electrolyte. This is explained by the losses in mechanical properties and the increase in surface roughness. As the evaluation period increases, the dissolution of the coating increases.

4. CONCLUSIONS

The systems are compared using the technique of electrochemical impedance spectroscopy in an evaluation period ending at 2160 hours; it is generally observed that the total impedance decreases. This is due to the topographic change generated by the wear phenomenon, which proves that the friction coefficient also varies according to the evaluation time, thus generating a quantity of anodic and cathodic zones. According to the results of corrosion-erosion tests, no significant changes

were observed in the coatings immersed at 720 hours. This condition allows establishing a good adhesion of the films to the substrate. It is also possible to demonstrate that there is no dissolution of the coating. At 1440 hours a decrease in the mechanical properties measured by the coefficient of friction is obtained, the value is stabilized up until 2160 hours behaviour of which is similar to that observed at 1440 hours. In addition, a good performance of the coatings was determined when they are submitted to a combined effect of tribology and corrosion. It was established that the coefficient of friction and the speed of the corrosion current have a tendency which indicates that β -TCP coatings have adequate electrochemical properties in the selected deposition conditions. This was attributed to the homogeneity of the surface, opening the possibility of using systems conformed by protective materials in biocompatibility applications and devices that are exposed to mechanical wear through corrosive mediums.

Acknowledgements

Dr Willian Aperador thanks the "Vicerrectoría de Investigaciones de la Universidad Militar Nueva Granada" project number ING-2992, validity 2019.

Author Contributions: Willian Aperador performed the obtaining coatings; J. Bautista worked in measurements in SEM, XPS and XRD and performed the interpretation of the data and the respective analysis. Julio Caicedo performed measurements corrosion tests performed the interpretation of the data.

REFERENCES

- [1] C. Prati, M.G. Gandolfi, *Calcium silicate bioactive cements: Biological perspectives and clinical applications*, Dental Materials, vol. 31, iss. 4, pp. 351-370, 2015, doi: [10.1016/j.dental.2015.01.004](https://doi.org/10.1016/j.dental.2015.01.004)
- [2] A.H. Touny, M.M. Saleh, *Fabrication of biphasic calcium phosphates nanowhiskers by reflux approach*, Ceramics International, vol. 44, iss. 14, pp. 16543-16547, 2018, doi: [10.1016/j.ceramint.2018.06.075](https://doi.org/10.1016/j.ceramint.2018.06.075)
- [3] F.S. Souza, M.J.S. Matos, B.R.L. Galvão, A.F.C. Arapiraca, S.N. da Silva, I.P. Pinheiro, *Adsorption of CO₂ on biphasic and amorphous calcium phosphates: An experimental and theoretical analysis*, Chemical Physics Letters, vol. 714, pp. 143-148, 2019, doi: [10.1016/j.cplett.2018.10.080](https://doi.org/10.1016/j.cplett.2018.10.080)
- [4] M. Furko, E.D. Bella, M. Fini, C. Balázs, *Corrosion and biocompatibility examination of multi-element modified calcium phosphate bioceramic layers*, Materials Science and Engineering: C, vol. 95, pp. 381-388, 2019, doi: [10.1016/j.msec.2018.01.010](https://doi.org/10.1016/j.msec.2018.01.010)
- [5] B. Gabbasov, M. Gafurov, A. Starshova, D. Shurtakova, F. Murzakhanov, G. Mamin, S. Orlinskii, *Conventional, pulsed and high-field electron paramagnetic resonance for studying metal impurities in calcium phosphates of biogenic and synthetic origins*, Journal of Magnetism and Magnetic Materials, vol. 470, pp. 109-117, 2019, doi: [10.1016/j.jmmm.2018.02.039](https://doi.org/10.1016/j.jmmm.2018.02.039)
- [6] J. Xiao, A.V. Rogachev, V.A. Yarmolenko, A.A. Rogachev, Y. Liu, X. Jiang, D. Sun, M.A. Yarmolenko, *Formation features, structure and properties of bioactive coatings based on phosphate-calcium layers, deposited by a low energy electron beam*, Surface and Coatings Technology, vol. 359, pp. 6-15, 2019, doi: [10.1016/j.surfcoat.2018.12.51](https://doi.org/10.1016/j.surfcoat.2018.12.51)
- [7] L. Zhang, C. Zhang, R. Zhang, D. Jiang, Q. Zhu, S. Wang, *Extraction and characterization of HA/ β -TCP biphasic calcium phosphate from marine fish*, Materials Letters, vol. 236, pp. 680-682, 2019, doi: [10.1016/j.matlet.2018.11.014](https://doi.org/10.1016/j.matlet.2018.11.014)
- [8] R. Chakraborty, S. Sengupta, P. Saha, K. Das, S. Das, *Synthesis of calcium hydrogen phosphate and hydroxyapatite coating on SS316 substrate through pulsed electrodeposition*, Materials Science and Engineering: C, vol. 69, pp. 875-883, 2016, doi: [10.1016/j.msec.2016.07.044](https://doi.org/10.1016/j.msec.2016.07.044)
- [9] Z. Zhou, J. Ruan, Z. Zhou, X. Shen, *Bioactivity of bioresorbable composite based on bioactive glass and poly-L-lactide*, Transactions of Nonferrous Metals Society of China, vol. 17, iss. 2, pp. 394-399, 2007, doi: [10.1016/S1003-6326\(07\)60105-8](https://doi.org/10.1016/S1003-6326(07)60105-8)
- [10] R.M. Castro, L.C.C. Cavaler, F.M. Marques, V.M. Bristot, A.S. Rocha, *Comparative of the Tribological Performance of Hydraulic Cylinders Coated by the Process of Thermal Spray HVOF and Hard Chrome Plating*, Tribology in Industry, vol. 36, no. 1, pp. 79-89, 2014.
- [11] W. Yi, X. Sun, D. Niu, X. Hu, *In vitro bioactivity of 3D Ti-mesh with bioceramic coatings in simulated body fluid*, Journal of Asian Ceramic Societies, vol. 2, iss. 3, pp. 210-214, 2014, doi: [10.1016/j.jascer.2014.04.002](https://doi.org/10.1016/j.jascer.2014.04.002)
- [12] D.M. Miskovic, K. Pohl, N. Birbilis, K.J. Laws, M. Ferry, *Formation of a phosphate conversion coating on bioresorbable Mg-based metallic glasses and its effect on corrosion performance*, Corrosion Science, vol. 129, pp. 214-225, 2017, doi: [10.1016/j.corsci.2017.10.014](https://doi.org/10.1016/j.corsci.2017.10.014)

- [13] S. Aktug, I. Kutbay, M. Usta, *Characterization and formation of bioactive hydroxyapatite coating on commercially pure zirconium by micro arc oxidation*, Journal of Alloys and Compounds, vol 695, pp. 998-1004, 2017, doi: [10.1016/j.jallcom.2016.10.217](https://doi.org/10.1016/j.jallcom.2016.10.217)
- [14] S.V. Dorozhkin, *Calcium orthophosphate deposits: Preparation, properties and biomedical applications*, Materials Science and Engineering: C, vol. 55, pp. 272-326, 2015, doi: [10.1016/j.msec.2015.05.033](https://doi.org/10.1016/j.msec.2015.05.033)
- [15] F. Errassifi, S. Sarda, A. Barroug, A. Legrouri, H. Sfihi, C. Rey, *Infrared, Raman and NMR investigations of risedronate adsorption on nanocrystalline apatites*, Journal of Colloid and Interface Science, vol. 420, pp. 101-111, 2014, doi: [10.1016/j.jcis.2014.01.017](https://doi.org/10.1016/j.jcis.2014.01.017)
- [16] B.C. Behera, S.K. Singdevsachan, R.R. Mishra, S.K. Dutta, H.N. Thatoi, *Diversity, mechanism and biotechnology of phosphate solubilising microorganism in mangrove—A review*, Biocatalysis and Agricultural Biotechnology, vol. 3, iss. 2, pp. 97-110, 2014, doi: [10.1016/j.bcab.2013.09.008](https://doi.org/10.1016/j.bcab.2013.09.008)
- [17] Q. Zhu, Z. Ablikim, T. Chen, Q. Cai, J. Xia, D. Jiang, S. Wang, *The preparation and characterization of HA/ β -TCP biphasic ceramics from fish bones*, Ceramics International, vol. 43, iss. 15, pp. 12213-12220, 2017, doi: [10.1016/j.ceramint.2017.06.082](https://doi.org/10.1016/j.ceramint.2017.06.082)
- [18] R.R. Behera, A. Das, D. Pamu, L.M. Pandey, M.R. Sankar, *Mechano-tribological properties and in vitro bioactivity of biphasic calcium phosphate coating on Ti-6Al-4V*, Journal of the Mechanical Behavior of Biomedical Materials, vol. 86, pp. 143-157, 2018, doi: [10.1016/j.jmbbm.2018.06.020](https://doi.org/10.1016/j.jmbbm.2018.06.020)
- [19] M. Bohner, G. Baroud, A. Bernstein, N. Döbelin, L. Galea, B. Hesse, R. Heuberger, S. Meille, P. Michel, B. von Rechenberg, J. Sague, Howard Seeherman, *Characterization and distribution of mechanically competent mineralized tissue in micropores of β -tricalcium phosphate bone substitutes*, Materials Today, vol. 20, iss. 3, pp. 106-115, 2017, doi: [10.1016/j.mattod.2017.02.002](https://doi.org/10.1016/j.mattod.2017.02.002)
- [20] R.R. Behera, A. Das, D. Pamu, L.M. Pandey, M.R. Sankar, *Mechano-tribological properties and in vitro bioactivity of biphasic calcium phosphate coating on Ti-6Al-4V*, Journal of the Mechanical Behavior of Biomedical Materials, vol. 86, pp. 143-157, 2018, doi: [10.1016/j.jmbbm.2018.06.020](https://doi.org/10.1016/j.jmbbm.2018.06.020)
- [21] K. Shim, H. Kim, S. Kim, K. Park, *Simple surface biofunctionalization of biphasic calcium phosphates for improving osteogenic activity and bone tissue regeneration*, Journal of Industrial and Engineering Chemistry, vol. 68, pp. 220-228, 2018, doi: [10.1016/j.jiec.2018.07.048](https://doi.org/10.1016/j.jiec.2018.07.048)
- [22] C. Damia, D. Marchat, C. Lemoine, N. Douard, V. Chaleix, V. Sol, N. Larochette, D. Logeart-Avramoglou, J. Brie, E. Champion, *Functionalization of phosphocalcic bioceramics for bone repair applications*, Materials Science and Engineering: C, vol. 95, pp. 343-354, 2019, doi: [10.1016/j.msec.2018.01.008](https://doi.org/10.1016/j.msec.2018.01.008)
- [23] H.S. Sofi, R. Ashraf, A. Khan, M.A. Beigh, S. Majeed, F.A. Sheikh, *Reconstructing nanofibers from natural polymers using surface functionalization approaches for applications in tissue engineering, drug delivery and biosensing devices*, Materials Science and Engineering: C, vol. 94, pp. 1102-1124, 2019, doi: [10.1016/j.msec.2018.10.069](https://doi.org/10.1016/j.msec.2018.10.069)
- [24] C. Adlhart, J. Verran, N.F. Azevedo, H. Olmez, M.M. Keinänen-Toivola, I. Gouveia, L.F. Melo, F. Crijns, *Surface modifications for antimicrobial effects in the healthcare setting: a critical overview*, Journal of Hospital Infection, vol. 99, iss. 3, pp. 239-249, 2018, doi: [10.1016/j.jhin.2018.01.018](https://doi.org/10.1016/j.jhin.2018.01.018)
- [25] M. Pourbaix, *Electrochemical corrosion of metallic biomaterials*, Biomaterials, vol. 5, iss. 3, pp. 122-134, 1984, doi: [10.1016/0142-9612\(84\)90046-2](https://doi.org/10.1016/0142-9612(84)90046-2)
- [26] X. Zhao, C. Liu, *Efficient removal of heavy metal ions based on the selective hydrophilic channels*, Chemical Engineering Journal, vol. 359, pp. 1644-1651, 2019, doi: [10.1016/j.cej.2018.10.229](https://doi.org/10.1016/j.cej.2018.10.229)
- [27] A. Mina, H.H. Caicedo, J.A. Uquillas, W. Aperador, O. Gutiérrez, J.C. Caicedo, *Biocompatibility behavior of β -tricalcium phosphate-chitosan coatings obtained on 316L stainless steel*, Materials Chemistry and Physics, vol. 175, pp. 68-80, 2016, doi: [10.1016/j.matchemphys.2016.02.070](https://doi.org/10.1016/j.matchemphys.2016.02.070)
- [28] Q. Yuan, Y. Huang, D. Liu, M. Chen, *Effects of solidification cooling rate on the corrosion resistance of a biodegradable β -TCP/Mg-Zn-Ca composite*, Bioelectrochemistry, vol. 124, pp. 93-104, 2018, doi: [10.1016/j.bioelechem.2018.07.005](https://doi.org/10.1016/j.bioelechem.2018.07.005)
- [29] Y. He, Y. Zhang, Y. Jiang, R. Zhou, J. Zhang, *Microstructure evolution, electrochemical properties and in-vitro properties of Ti-Nb-Zr based biocomposite by hydroxyapatite bioceramic*, Journal of Alloys and Compounds, vol. 764, pp. 987-1002, 2018, doi: [10.1016/j.jallcom.2018.06.132](https://doi.org/10.1016/j.jallcom.2018.06.132)
- [30] P. Guzmán, L. Yate, M. Sandoval, J. Caballero, W. Aperador, *Characterization of the Micro-Abrasive Wear in Coatings of TaC-HfC/Au for Biomedical Implants*, Materials, vol. 10, iss. 8, pp. 842-849, 2017, doi: [10.3390/ma10080842](https://doi.org/10.3390/ma10080842)
- [31] S.R. Paital, N.B. Dahotre, *Calcium phosphate coatings for bio-implant applications: Materials, performance factors, and methodologies*, Materials Science and Engineering: R: Reports, vol. 66, iss. 1-3, pp. 1-70, 2009, doi: [10.1016/j.mser.2009.05.001](https://doi.org/10.1016/j.mser.2009.05.001)

- [32] A.K. Tran, A. Sapkota, J. Wen, J. Li, M. Takei, *Linear relationship between cytoplasm resistance and hemoglobin in red blood cell hemolysis by electrical impedance spectroscopy & eight-parameter equivalent circuit*, Biosensors and Bioelectronics, vol. 119, pp. 103-109, 2018, doi: [10.1016/j.bios.2018.08.012](https://doi.org/10.1016/j.bios.2018.08.012)
- [33] W. Piedrahita, J.C. Caicedo, W. Aperador, *Tribological and Electrochemical Properties of AISI D3 Steel Coated with Hafnium Carbon Nitride*, Tribology in Industry, vol. 40, no. 3, pp. 488-500, 2018, doi: [10.24874/ti.2018.40.03.14](https://doi.org/10.24874/ti.2018.40.03.14)
- [34] K.P. Ananth, A.J. Nathanael, S.P. Jose, T.H. Oh, D. Mangalaraj, A.M. Ballamurugan, *Controlled electrophoretic deposition of HAp/ β -TCP composite coatings on piranha treated 316L SS for enhanced mechanical and biological properties*, Applied Surface Science, vol. 353, pp. 189-199, 2015, doi: [10.1016/j.apsusc.2015.06.111](https://doi.org/10.1016/j.apsusc.2015.06.111)
- [35] U. Gbureck, O. Grolms, J.E. Barralet, L.M. Grover, R. Thull, *Mechanical activation and cement formation of β -tricalcium phosphate*, Biomaterials, vol. 24, iss. 23, pp. 4123-4131, 2003, doi: [10.1016/S0142-9612\(03\)00283-7](https://doi.org/10.1016/S0142-9612(03)00283-7)